

Interpolating 't Hooft model between the Instant Form Dynamics and the Light Front Dynamics

Bailing Ma

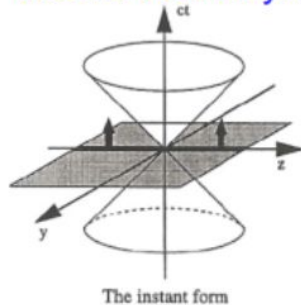
Light Cone 2022 Online: Physics of Hadrons on the Light Front

Sep. 21, 2022

Light Front Dynamics

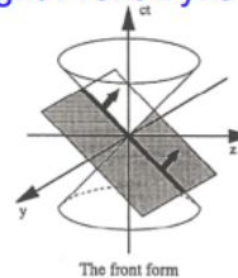
IFD

Instant Form Dynamics



LFD

Light-Front Dynamics

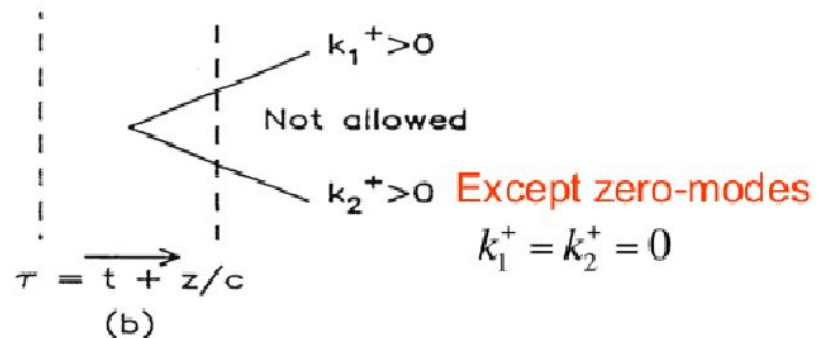
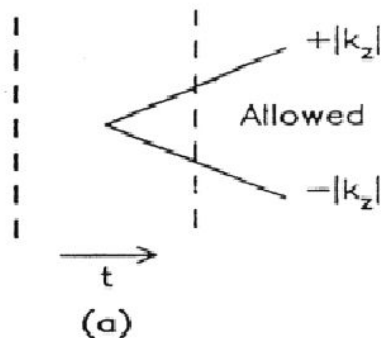


Energy-Momentum Dispersion Relations

$$p^0 = \sqrt{\vec{p}^2 + m^2}$$

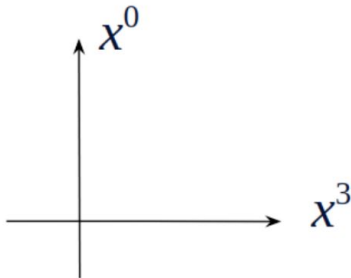
$$p^- = \frac{p_\perp^2 + m^2}{p^+}$$

Time-ordered Diagrams: Vacuum fluctuations



Interpolation Method

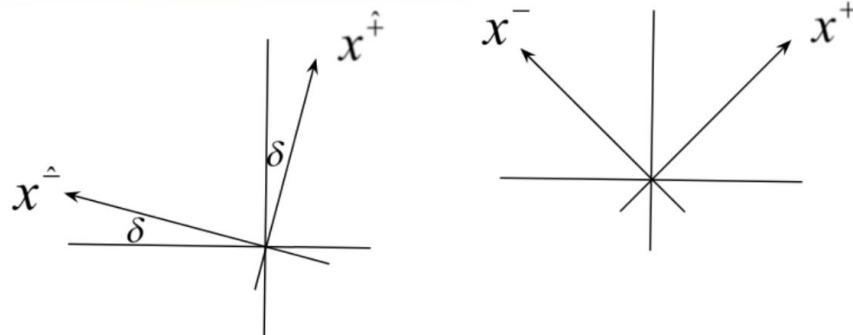
IFD



$$(IFD) \quad 0 \leq \delta \leq \frac{\pi}{4} \quad (LFD)$$

$$1 \geq C \equiv \cos(2\delta) \geq 0$$

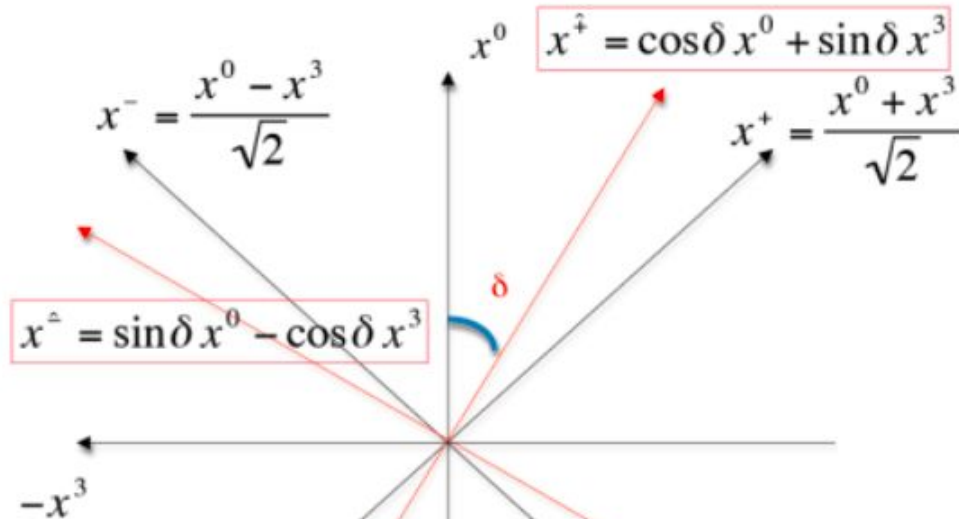
LFD



$$\begin{pmatrix} x^{\hat{+}} \\ x^{\hat{1}} \\ x^{\hat{2}} \\ x^{\hat{-}} \end{pmatrix} = \begin{pmatrix} \cos \delta & 0 & 0 & \sin \delta \\ 0 & 1 & 0 & 0 \\ 0 & 0 & 1 & 0 \\ \sin \delta & 0 & 0 & -\cos \delta \end{pmatrix} \begin{pmatrix} x^0 \\ x^1 \\ x^2 \\ x^3 \end{pmatrix}$$

- Relate IFD and LFD, show the whole landscape in between
- Magnify LF zero mode by varying the δ parameter
- Clarify any conceivable confusion between the IMF and LFD

Works on Interpolation between IFD and LFD



K. Hornbostel, PRD45, 3781 (1992) – RQFT
C.Ji and S.Rey, PRD53,5815(1996) – Chiral Anomaly
C.Ji and C. Mitchell, PRD64,085013 (2001) – Poincare Algebra
C.Ji and A. Suzuki, PRD87,065015 (2013) – Scattering Amps
C.Ji, Z. Li and A. Suzuki, PRD91, 065020 (2015) – EM Gauges
Z.Li, M. An and C.Ji, PRD92, 105014 (2015) – Spinors
C.Ji, Z.Li, B.Ma and A.Suzuki, PRD98, 036017(2018) – QED
B.Ma and C.Ji, PRD104, 036004(2021) – QCD₁₊₁

't Hooft model vs IFD QCD₃₊₁

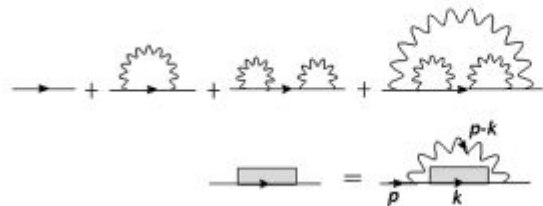
$$\mathcal{L} = -\frac{1}{4} F_{\hat{\mu}\hat{\nu}}^a F^{\hat{\mu}\hat{\nu}a} + \bar{\psi}(i\gamma^{\hat{\mu}} D_{\hat{\mu}} - m)\psi,$$

$$D_{\hat{\mu}} = \partial_{\hat{\mu}} - ig A_{\hat{\mu}}^a t_a$$

$$F_{\hat{\mu}\hat{\nu}}^a = \partial_{\hat{\mu}} A_{\hat{\nu}}^a - \partial_{\hat{\nu}} A_{\hat{\mu}}^a + g f^{abc} A_{\hat{\mu}}^b A_{\hat{\nu}}^c.$$

- 1 space 1 time dimensions, where confinement arises naturally due to the linear potential.
- Large N_c ('t Hooft coupling $\lambda \sim g^2 N_c$ is kept finite while $N_c \rightarrow \infty$ and $g \rightarrow 0$), so that non-planar diagrams are negligible. (Dimensionful quantities are scaled with respect to $\sqrt{2\lambda}$.)
- Gluon self-couplings are absent, and there is no ghost, with the use of axial gauge.

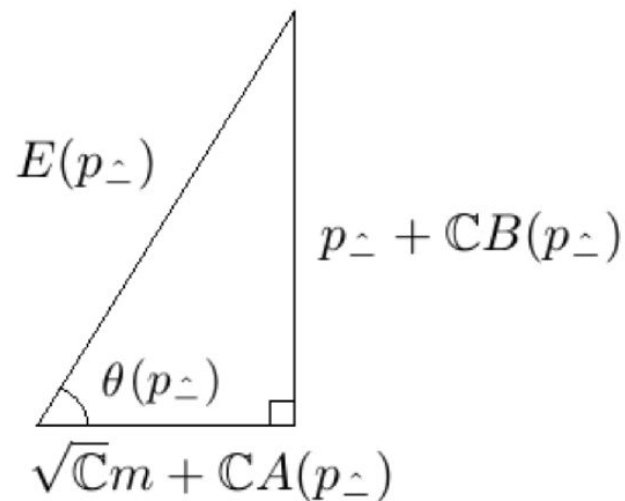
Mass gap equation



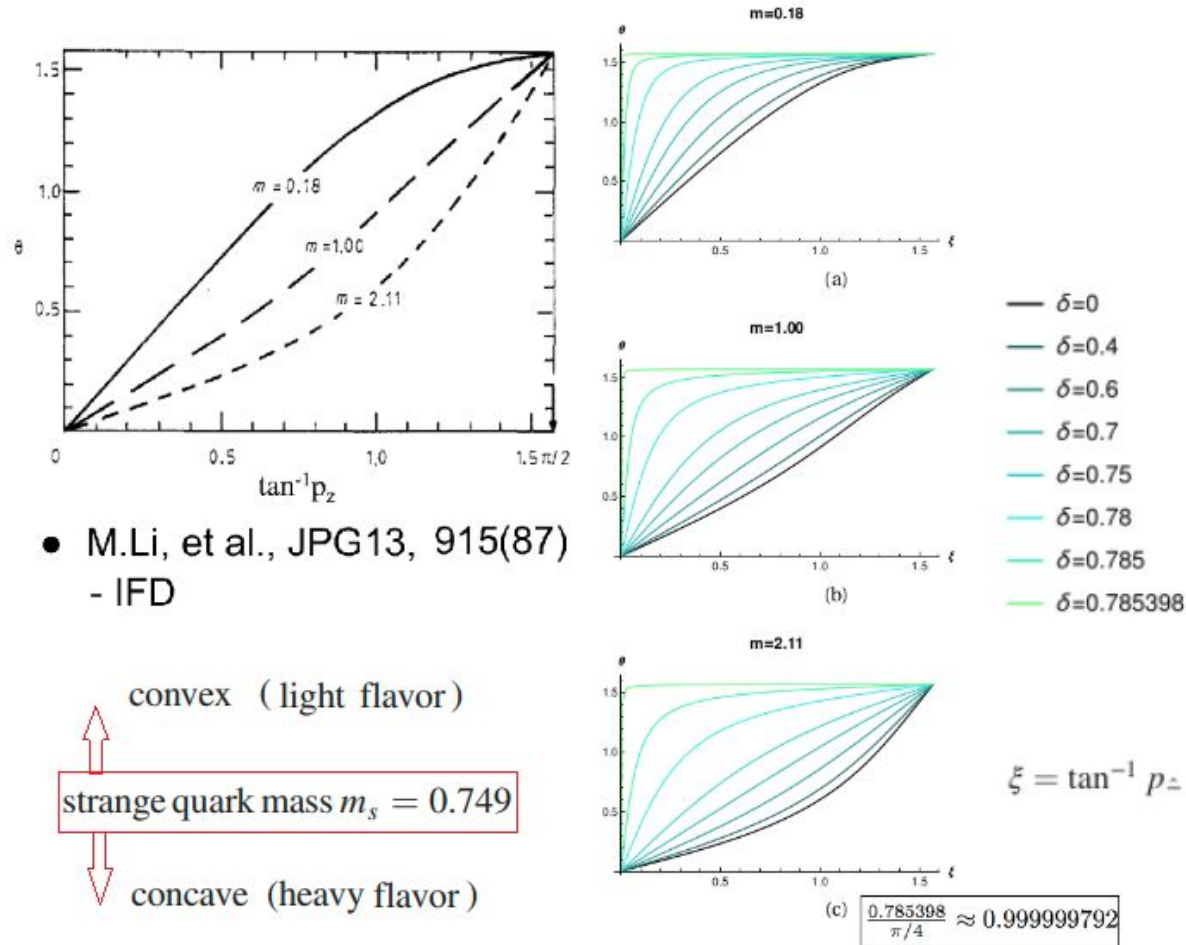
$$\Sigma(p_{\perp}) = \sqrt{\mathbb{C}}A(p_{\perp}) + \gamma_{\perp}B(p_{\perp})$$

$$E(p_{\perp})\cos\theta(p_{\perp}) = \sqrt{\mathbb{C}}m + \mathbb{C} \cdot \frac{\lambda}{2} \int \frac{dk_{\perp}}{(p_{\perp} - k_{\perp})^2} \cos\theta(k_{\perp})$$

$$E(p_{\perp})\sin\theta(p_{\perp}) = p_{\perp} + \mathbb{C} \cdot \frac{\lambda}{2} \int \frac{dk_{\perp}}{(p_{\perp} - k_{\perp})^2} \sin\theta(k_{\perp})$$



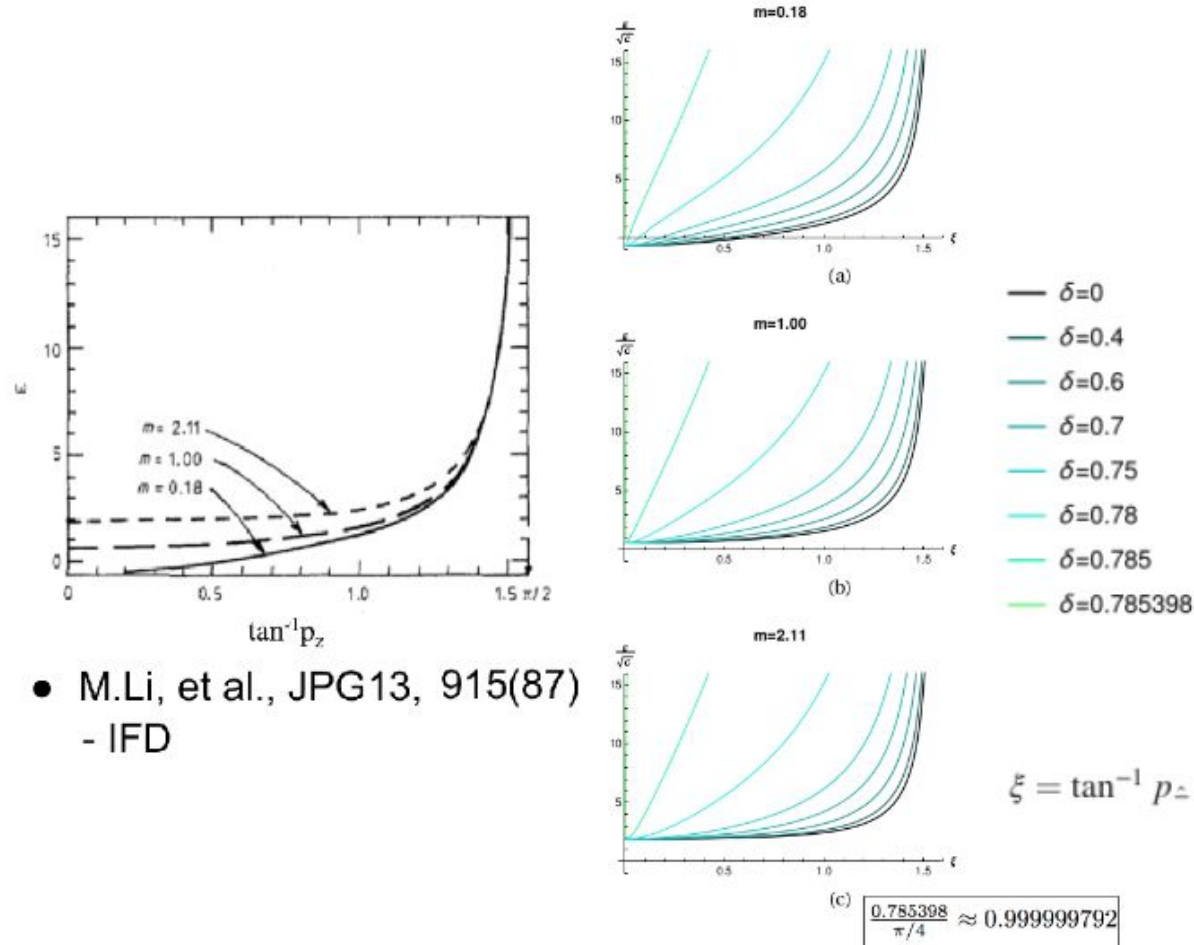
Solutions of the mass gap equation : θ



- M.Li, et al., JPG13, 915(87) - IFD

The numerical solutions of $\theta(p_z)$ for several interpolation angles, corresponding to the quark mass values in Figure 4 of Ref. Li et al. (1987). All the mass values are in the unit of $\sqrt{2\lambda}$. Note that $\theta(p_z)$ is an odd function of p_z and only the positive p_z range is plotted with the variable $\xi = \tan^{-1} p_z$.

Solutions of the mass gap equation : E



- M.Li, et al., JPG13, 915(87)
- IFD

The solutions of $E(p_z)/\sqrt{C}$ for several interpolation angles for different choices of quark mass corresponding to the quark mass values in Figure 5 of Ref. Li et al. (1987). All quantities are in proper units of $\sqrt{2\lambda}$. $E(p_z)$ is an even function of p_z . We plot only for positive p_z with the variable $\xi = \tan^{-1} p_z$.

Dressed quark propagator

Free Propagator

$$S_f(p) = \frac{1}{\not{p} - m + i\varepsilon}$$



Interacting Propagator

$$S(p) = \frac{1}{\not{p} - m - \Sigma(p) + i\varepsilon}$$

$$= \frac{F(p)}{\not{p} - M(p) + i\varepsilon}$$

$\Sigma(p) = \Sigma_s(p) + \Sigma_v(p)\not{p}$

$$F(p) = (1 - \Sigma_v(p))^{-1} \quad \text{“Wave function renormalization factor”}$$

$$M(p) = \frac{m + \Sigma_s(p)}{1 - \Sigma_v(p)} \quad \text{“Renormalized fermion mass function”}$$

Ji, C.-R. (2012). Pion loops in chiral perturbation theory and light-front dynamics. Few Body Syst., 52:421–426.

Energy-momentum dispersion relation for a dressed quark

Free particle
in IFD



Free particle
in interpolation



Dressed particle
in interpolation

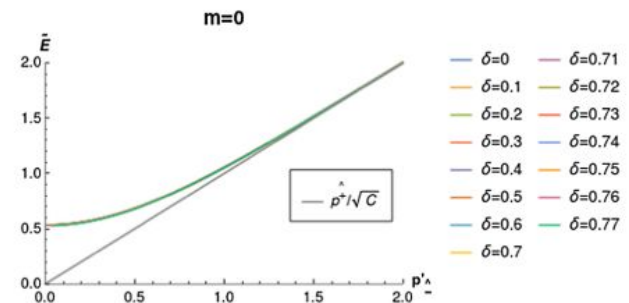
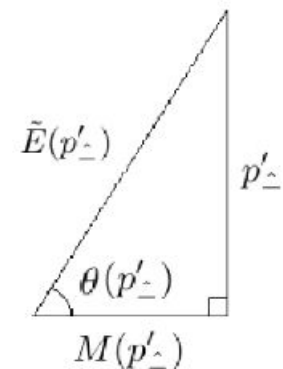
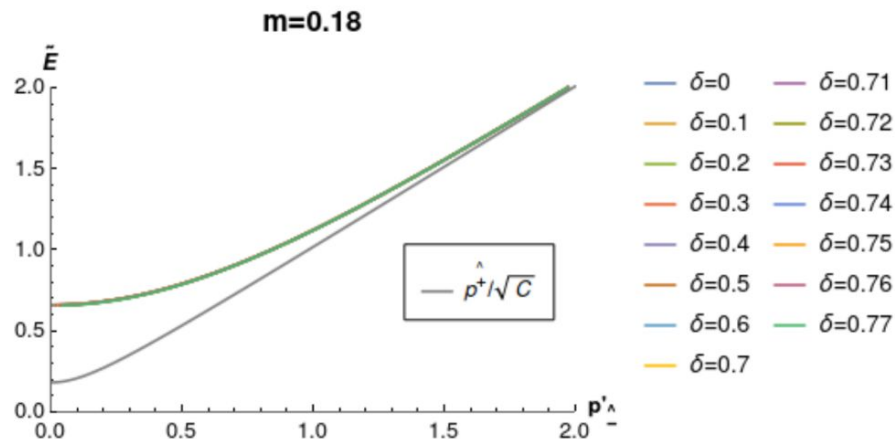
$$\frac{F(p'_\perp)E(p'_\perp)}{\sqrt{C}} = \sqrt{p'^2_\perp + M(p'_\perp)^2} \equiv \tilde{E}(p'_\perp)$$

$$E = \sqrt{m^2 + p_z^2}$$

$$p'^{\pm} = \sqrt{m^2 + p'^2_\perp}$$

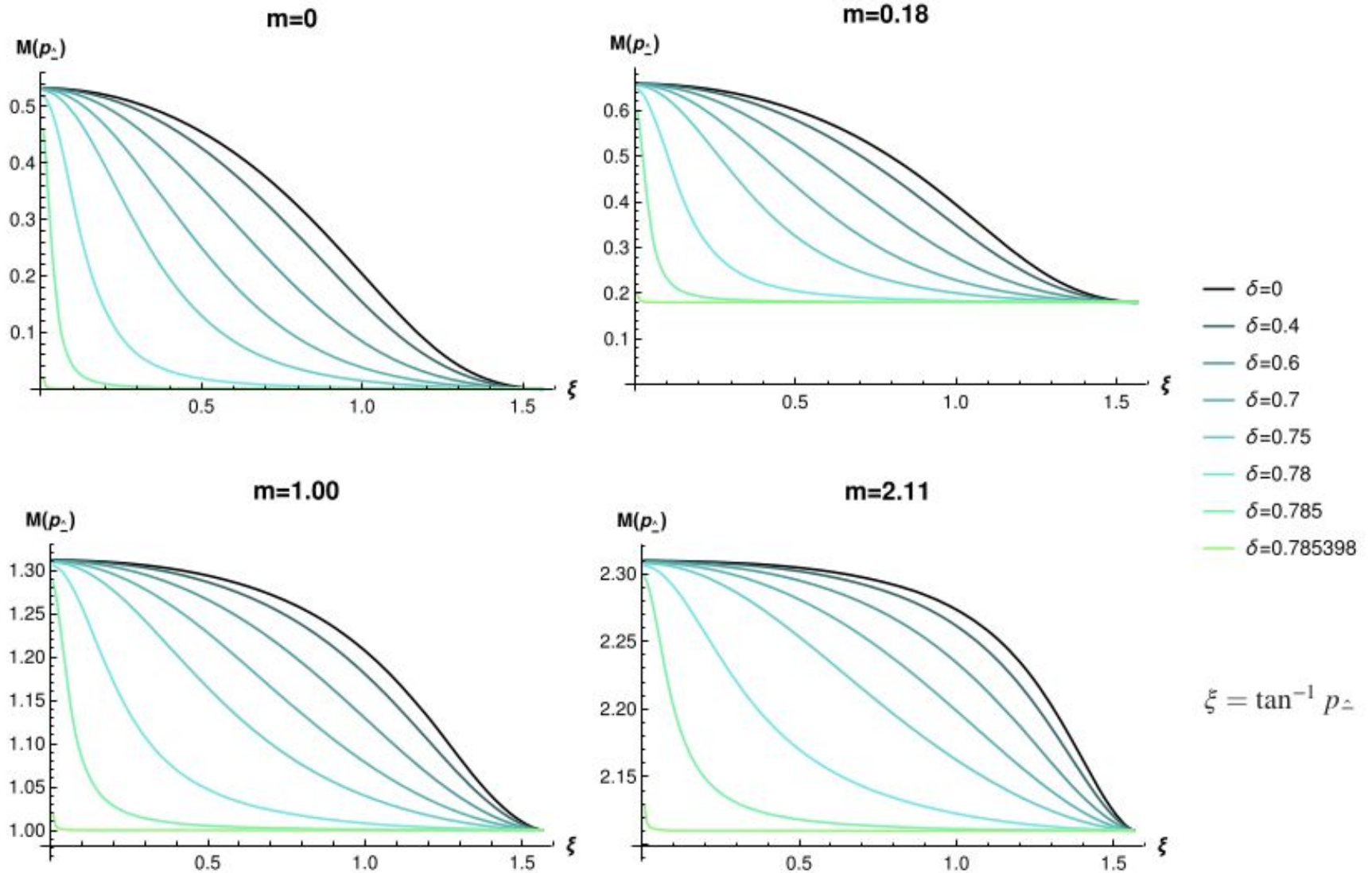
$$\tilde{E}(p'_\perp) = \sqrt{M(p'_\perp)^2 + p'^2_\perp}$$

where the interpolating rescaled variables $p'^{\pm} = \frac{p^{\pm}}{\sqrt{C}}$; $p'_\perp = \frac{p_\perp}{\sqrt{C}}$.

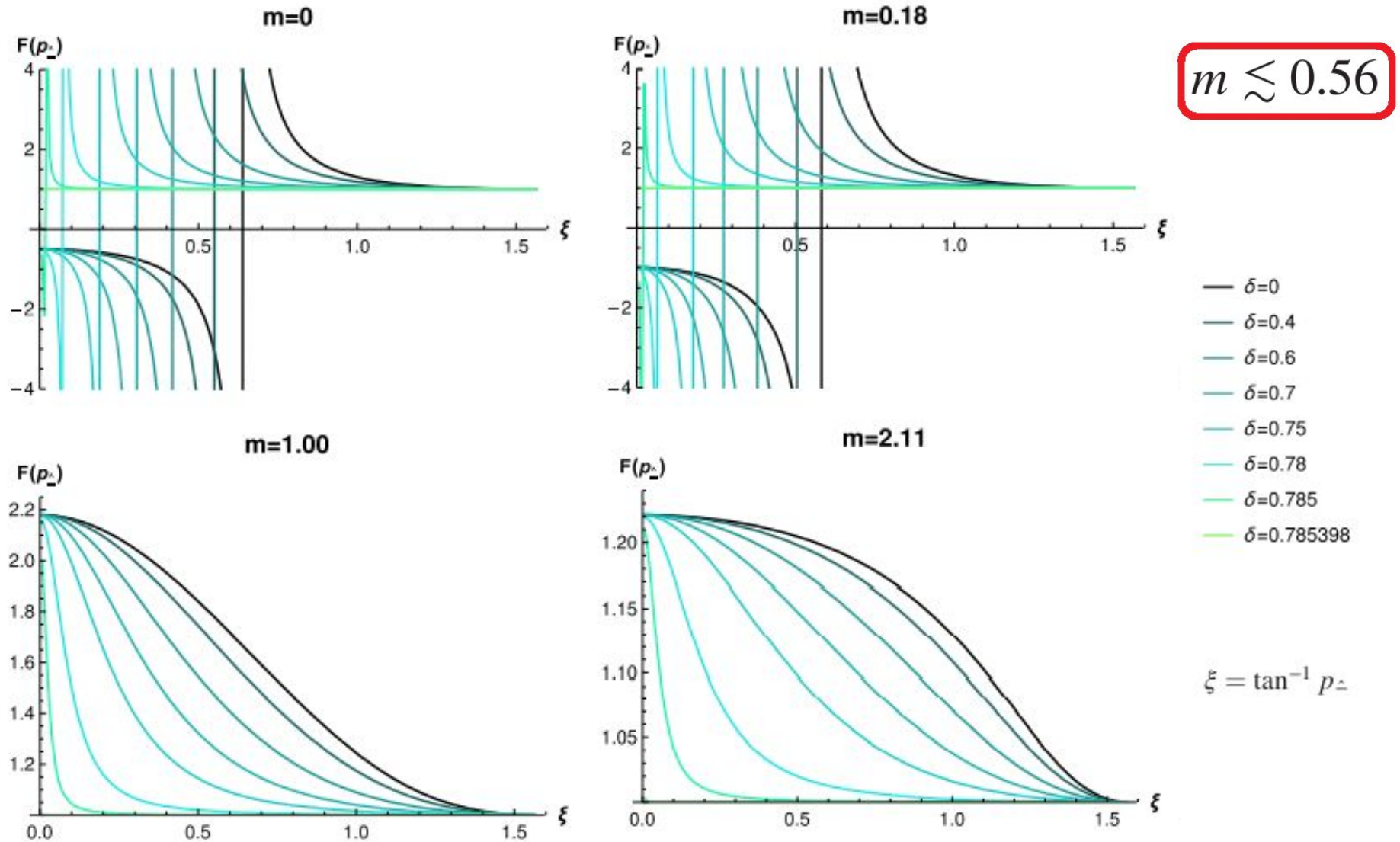


Confinement \longleftrightarrow Asymptotic freedom

Running quark mass function

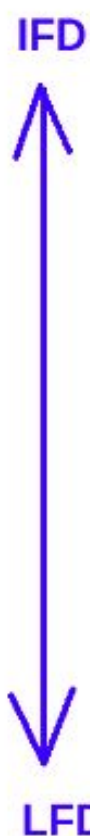


Wavefunction renormalization factor



Chiral condensate: zero mass case

$$\langle \bar{\psi}\psi \rangle|_{\text{ren}} = -\frac{N_c}{2\pi} \int_{-\infty}^{+\infty} dp'_z [\cos \theta(p'_z) - \cos \theta_f(p'_z)].$$



δ	number of grid points	$\langle \bar{\psi}\psi \rangle _{m \rightarrow 0}/N_c$
0	200	-0.285209
	600	-0.287508
0.4	200	-0.285164
	600	-0.287496
0.6	200	-0.284792
	600	-0.287375
0.7	200	-0.283836
	600	-0.287059
0.75	200	-0.281837
	600	-0.286396
0.78	200	-0.296575
	600	-0.291334
0.785	600	-0.298104
	1000	-0.294377
	3000	-0.290590
0.78535	1000	-0.304659
	3000	-0.294134
	5000	-0.291964

Analytic value is

$$-1/\sqrt{12} \approx -0.29$$

Burkardt, M. (1996).

Phys. Rev. D, 53:933–938.

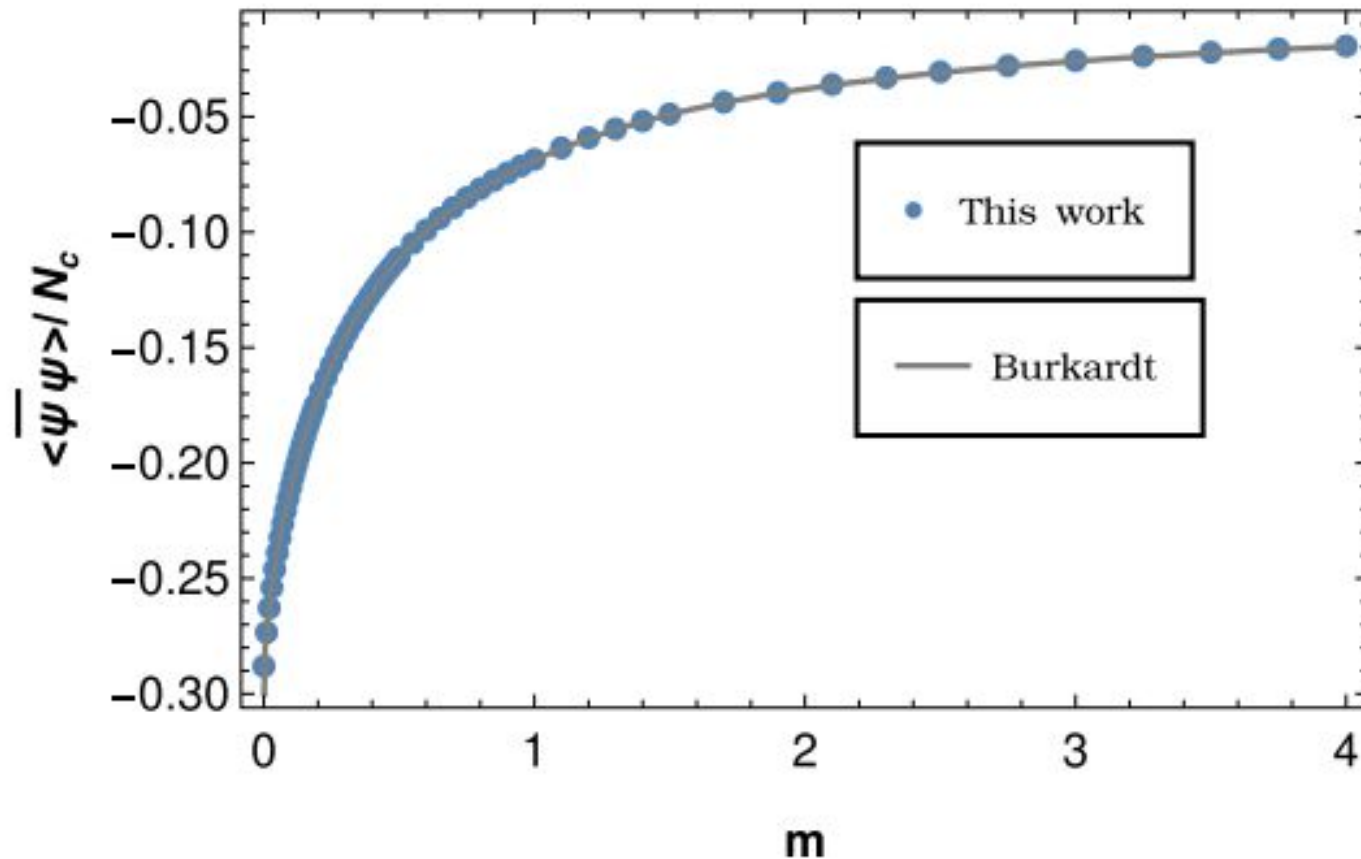
Zhitnitsky, A. R. (1985).

Phys. Lett. B, 165:405–409.

Zhitnitsky, A. R. (1996).

Phys. Rev. D, 53:5821–5833.

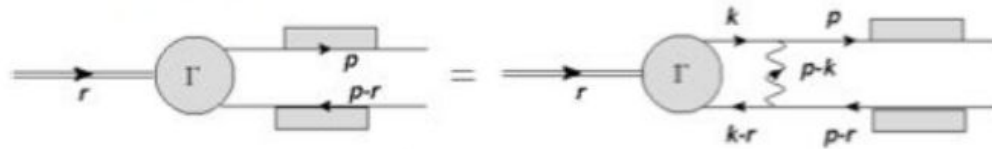
Chiral condensate: varying mass case



Numerical results of the condensation $\langle \bar{\psi}\psi \rangle|_{\text{ren}}$ as a function of m in comparison with the analytic result in M. Burkardt, *Phys. Rev. D* **53**, 933 (1996). All quantities are in proper units of $\sqrt{2\lambda}$.

Bound state equation

$$\Gamma(r, p) = \frac{i\lambda}{2\pi} \int \frac{dk_{\perp} dk_{\perp}^{\dagger}}{(p_{\perp} - k_{\perp})^2} S(p) \gamma^{\dagger} \Gamma(r, k) \gamma^{\dagger} S(p - r)$$



$$\begin{aligned} & \left[-r_{\perp} + \frac{-Sp_{\perp} + E(p_{\perp})}{\mathbb{C}} + \frac{S(p_{\perp} - r_{\perp}) + E(p_{\perp} - r_{\perp})}{\mathbb{C}} \right] \hat{\phi}_{+}(r_{\perp}, p_{\perp}) \\ &= \lambda \int \frac{dk_{\perp}}{(p_{\perp} - k_{\perp})^2} \left[C(p_{\perp}, k_{\perp}, r_{\perp}) \hat{\phi}_{+}(r_{\perp}, k_{\perp}) - S(p_{\perp}, k_{\perp}, r_{\perp}) \hat{\phi}_{-}(r_{\perp}, k_{\perp}) \right], \\ & \left[r_{\perp} + \frac{-S(p_{\perp} - r_{\perp}) + E(p_{\perp} - r_{\perp})}{\mathbb{C}} + \frac{Sp_{\perp} + E(p_{\perp})}{\mathbb{C}} \right] \hat{\phi}_{-}(r_{\perp}, p_{\perp}) \\ &= \lambda \int \frac{dk_{\perp}}{(p_{\perp} - k_{\perp})^2} \left[C(p_{\perp}, k_{\perp}, r_{\perp}) \hat{\phi}_{-}(r_{\perp}, k_{\perp}) - S(p_{\perp}, k_{\perp}, r_{\perp}) \hat{\phi}_{+}(r_{\perp}, k_{\perp}) \right]. \end{aligned}$$



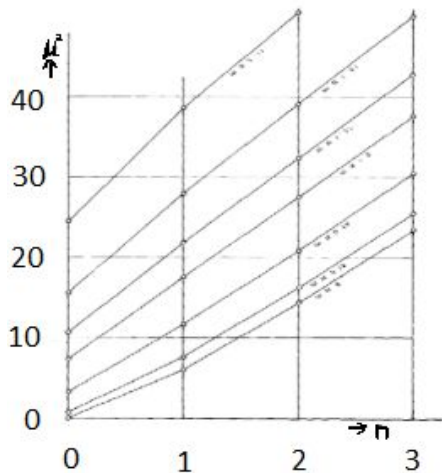
LFD

$$\left[\mathcal{M}^2 - \frac{m^2 - 2\lambda}{x} - \frac{m^2 - 2\lambda}{1 - x} \right] \phi(x) = -2\lambda \int_0^1 \frac{dy}{(x - y)^2} \phi(y)$$



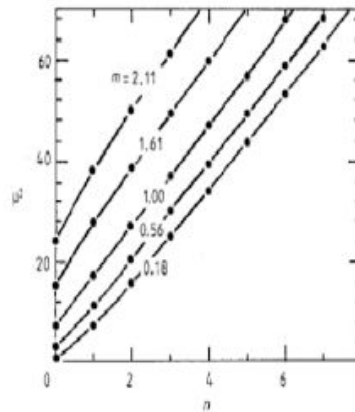
Meson spectroscopy

LFD



't Hooft, G. (1974).
Nucl. Phys. B, 75:461–470.

IFD

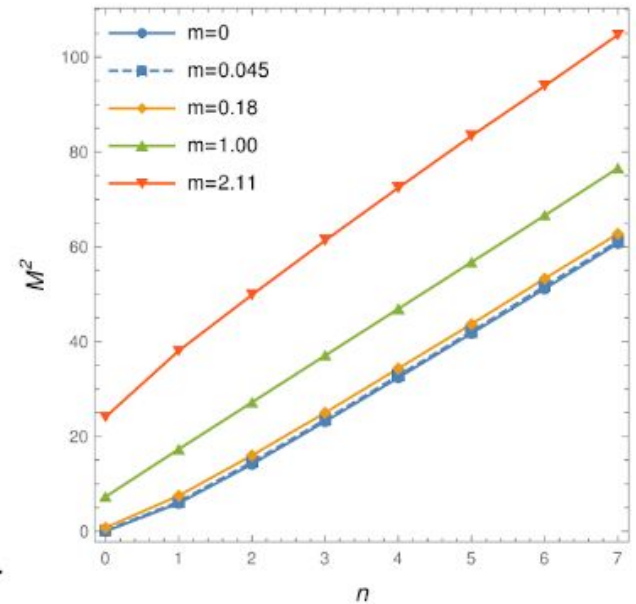


Bars, I. and Green, M. B. (1978).
Phys. Rev. D, 17:537–545.

Li, M., Willets, L., and Birse, M. C. (1987).
J. Phys. G, 13:915–923.

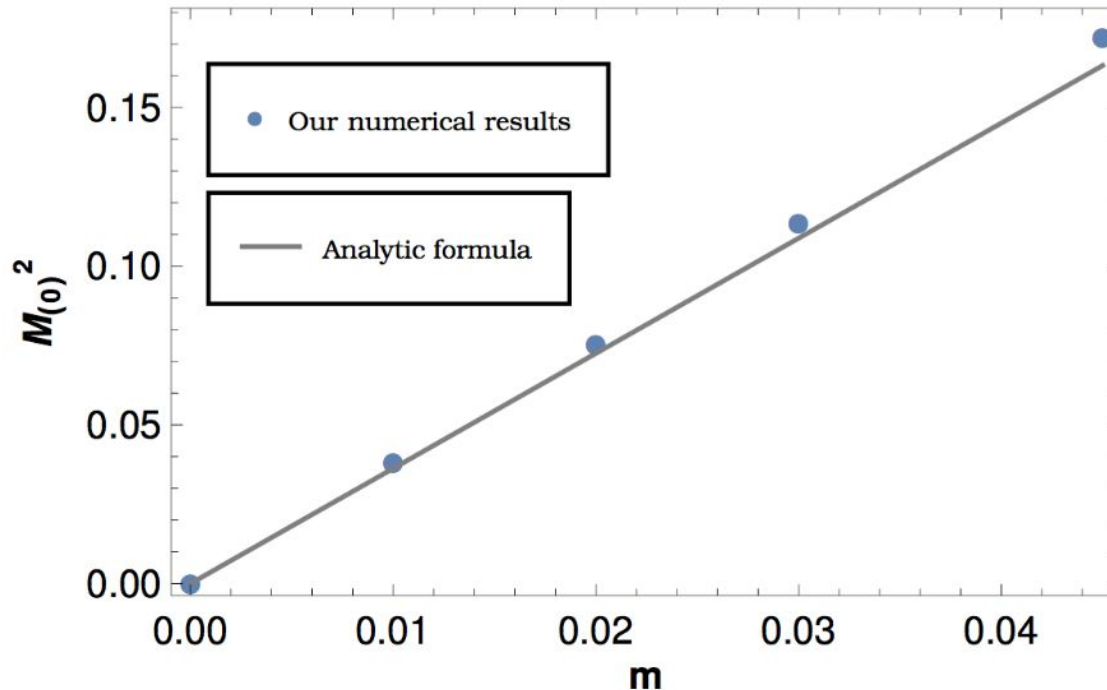
Jia, Y., Liang, S., Li, L., and Xiong, X. (2017).
JHEP, 11:151.

Interpolation form



Ma, B. and Ji, C.-R. (2021).
Phys. Rev. D, 104:036004.

Gell-Mann - Oakes - Renner relation



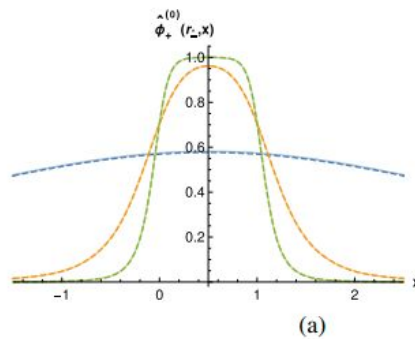
$$\mathcal{M}_{\pi}^2 = -\frac{4m \langle \bar{\psi}\psi \rangle}{f_{\pi}^2} = \sqrt{\frac{8\pi^2 m^2 \lambda}{3}} \quad f_{\pi} = \sqrt{N_c/\pi}$$

Brower, R. C., Spence, W. L., and Weis, J. H. (1979). Bound states and asymptotic limits for quantum chromodynamics in two dimensions. Phys. Rev. D, 19:3024–3049.

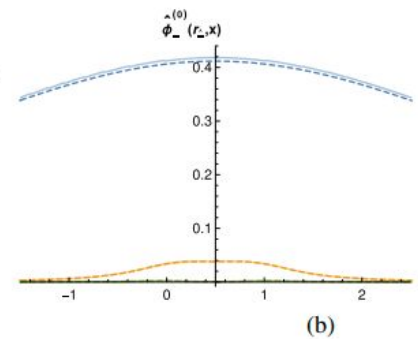
Wavefunction solutions

Ground state wave functions $\hat{\phi}_+^{(0)}(r_\perp, x)$ and $\hat{\phi}_-^{(0)}(r_\perp, x)$ for $m = 0$. All quantities are in proper units of $\sqrt{2\lambda}$.

IFD ($\delta=0$)



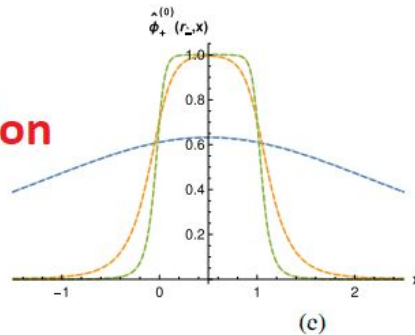
— $r_\perp = 0.2 M_{0,18}$, analytic
— $r_\perp = 2 M_{0,18}$, analytic
— $r_\perp = 5 M_{0,18}$, analytic
--- $r_\perp = 0.2 M_{0,18}$
--- $r_\perp = 2 M_{0,18}$
--- $r_\perp = 5 M_{0,18}$



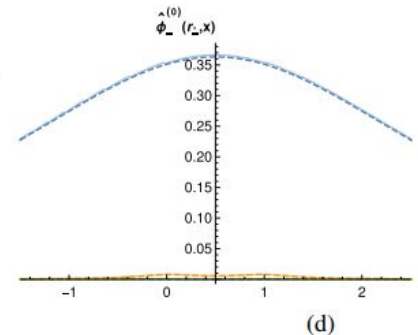
— $r_\perp = 0.2 M_{0,18}$, analytic
— $r_\perp = 2 M_{0,18}$, analytic
— $r_\perp = 5 M_{0,18}$, analytic
--- $r_\perp = 0.2 M_{0,18}$
--- $r_\perp = 2 M_{0,18}$
--- $r_\perp = 5 M_{0,18}$

Interpolation

($\delta=0.6$)



— $r_\perp = 0.2 M_{0,18}$, analytic
— $r_\perp = 2 M_{0,18}$, analytic
— $r_\perp = 5 M_{0,18}$, analytic
--- $r_\perp = 0.2 M_{0,18}$
--- $r_\perp = 2 M_{0,18}$
--- $r_\perp = 5 M_{0,18}$



— $r_\perp = 0.2 M_{0,18}$, analytic
— $r_\perp = 2 M_{0,18}$, analytic
— $r_\perp = 5 M_{0,18}$, analytic
--- $r_\perp = 0.2 M_{0,18}$
--- $r_\perp = 2 M_{0,18}$
--- $r_\perp = 5 M_{0,18}$

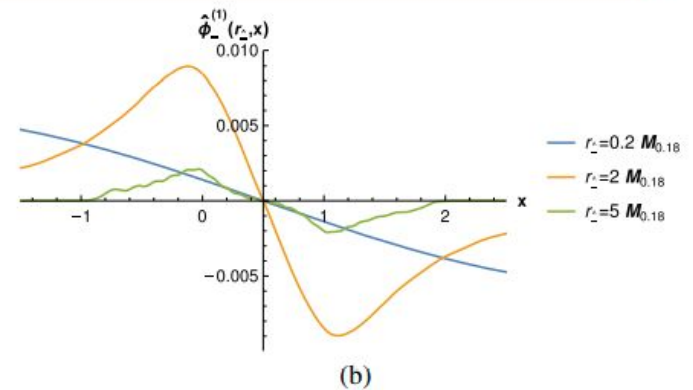
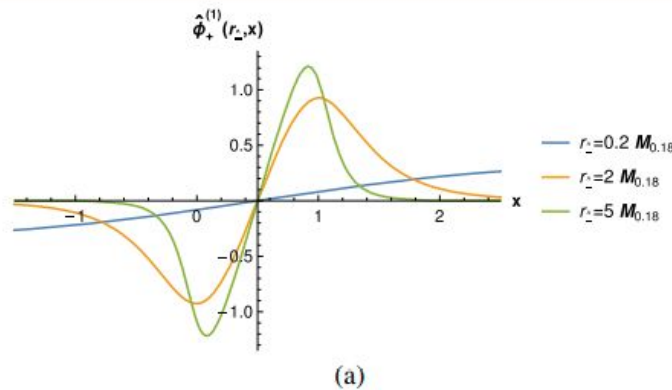
the analytic solution in the interpolating formulation is given by

$$\hat{\phi}_\pm^{(0)}(r_\perp, p_\perp) = \frac{1}{2} \left(\cos \frac{\theta(r_\perp - p_\perp) - \theta(p_\perp)}{2} \pm \sin \frac{\theta(r_\perp - p_\perp) + \theta(p_\perp)}{2} \right)$$

Wavefunction solutions

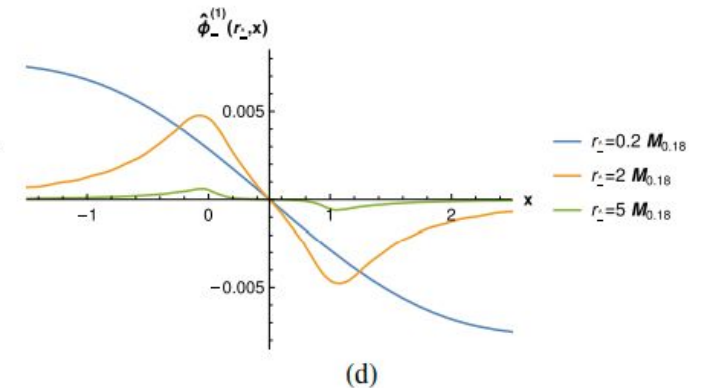
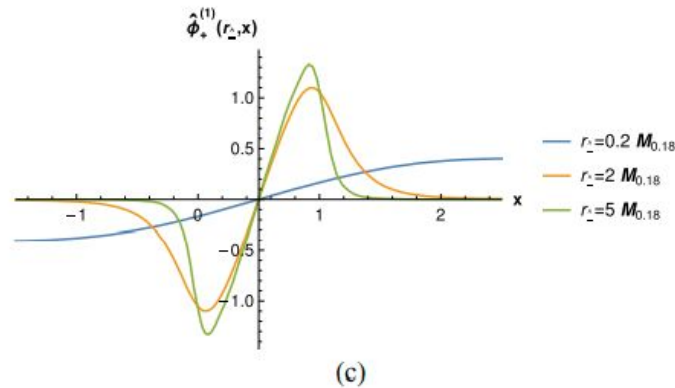
First excited state wave functions $\hat{\phi}_+^{(1)}(r_-, x)$ and $\hat{\phi}_-^{(1)}(r_-, x)$ for $m = 0$.

IFD ($\delta=0$)



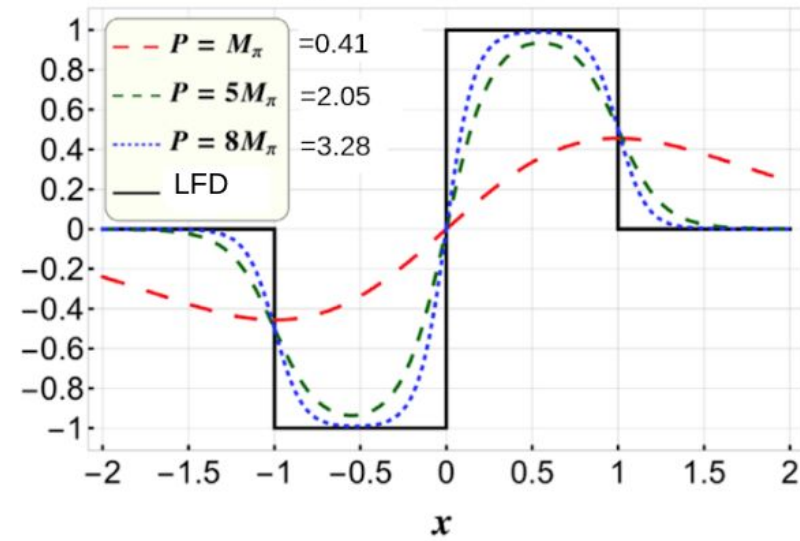
Interpolation

($\delta=0.6$)



Quasi-PDF

$\tilde{q}_0^{\pi_\chi}(x, P)$ and $q_0^{\pi_\chi}(x)$

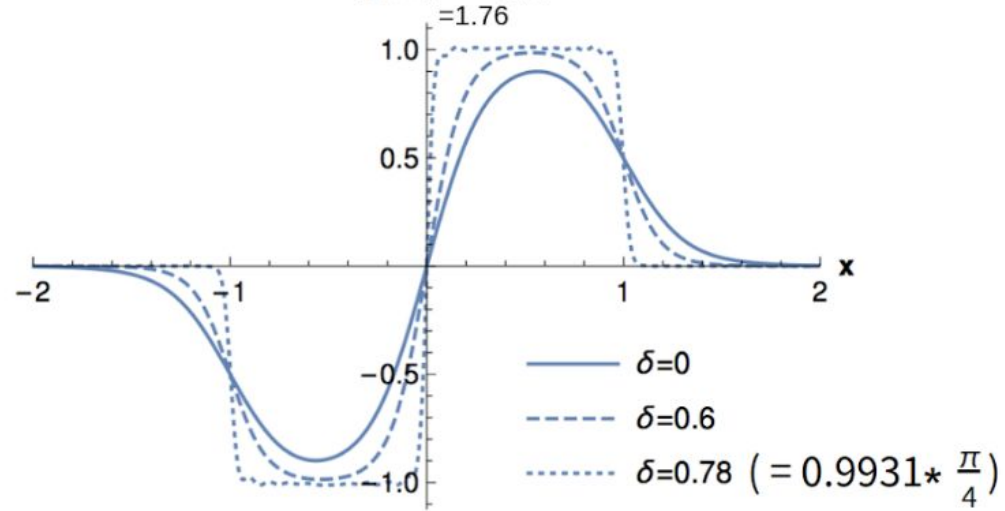


Quark quasi-PDFs and light-front PDF for the chiral pion.

All quantities are in proper units of $\sqrt{2\lambda}$.

Jia, Y., Liang, S., Xiong, X., and Yu, R. (2018). *Phys. Rev. D*, 98:054011.

$\tilde{q}_0(x, r_\perp = 2 M_{0.18})$



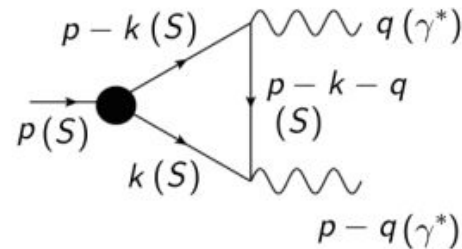
Interpolating "quasi-PDFs" for the chiral pion.

Ma, B. and Ji, C.-R. (2021). *Phys. Rev. D*, 104:036004.

Outlook

- Transition form factors in 1+1 dimensional models

- scalar loop
- fermion loop
- 't Hooft model



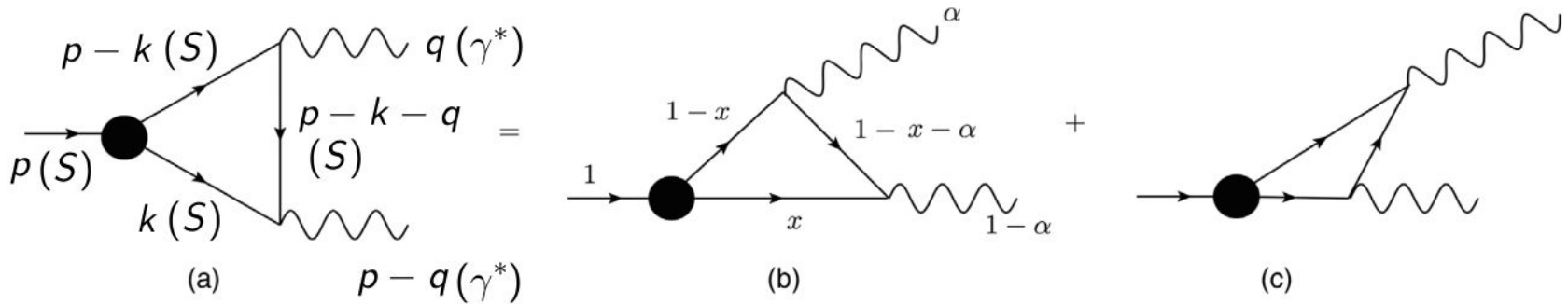
- Drell-Yan-West frame ($q^+ = 0$) can no longer be used, as it results in $q^2 = 0$.
- Choosing a $q^+ \neq 0$ frame, one can also directly access not only the space-like ($q^2 < 0$), but also the time-like ($q^2 > 0$) momentum regions.
- Define a parameter such that

$$p = (p^+, p^-) = \left(p^+, \frac{M^2}{2p^+} \right)$$

$$q = (q^+, q^-) = \left(\alpha p^+, \frac{M^2}{2p^+} - \frac{q'^2}{2(1-\alpha)p^+} \right)$$

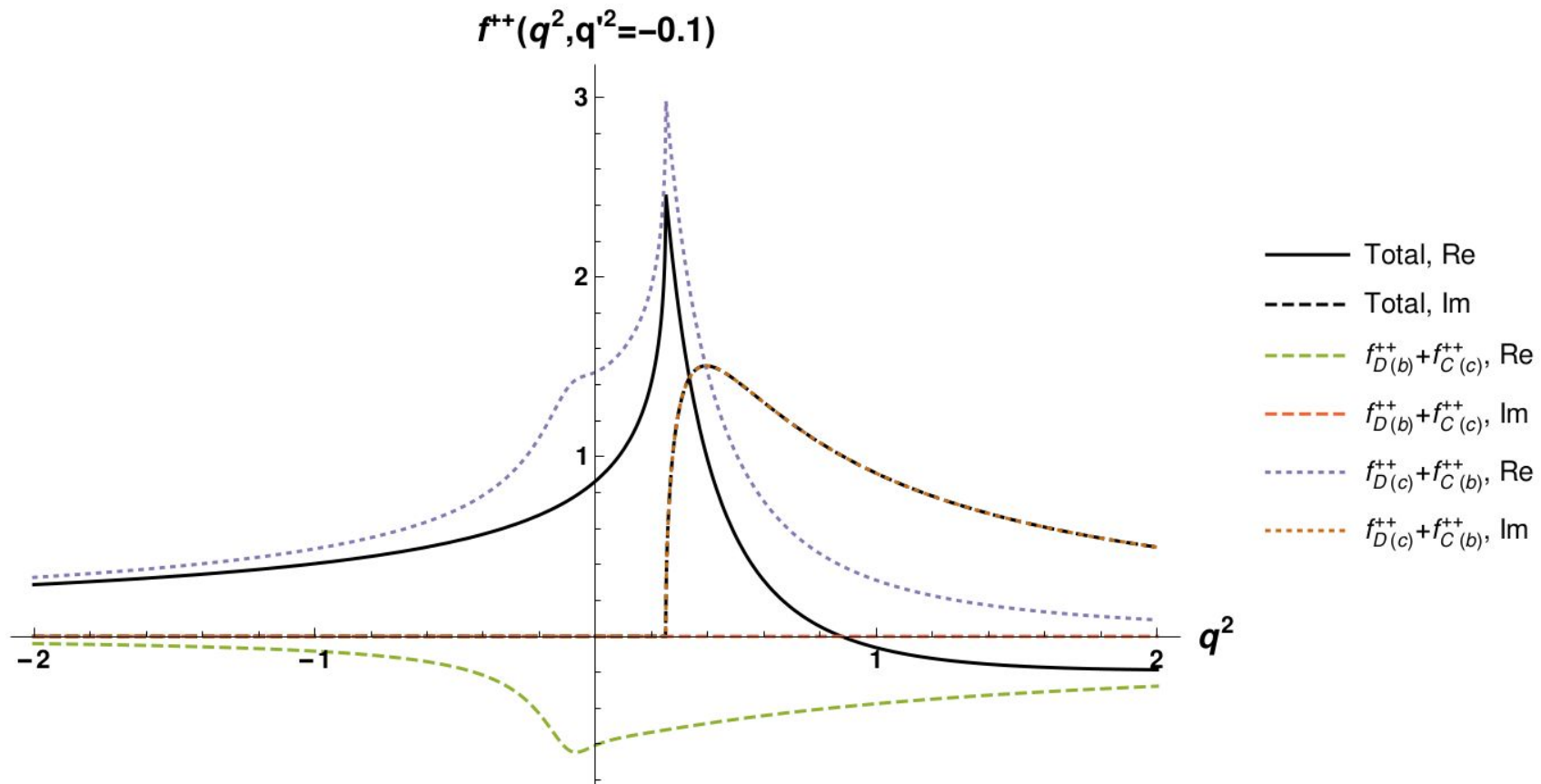
$$q' = p - q = (q'^+, q'^-) = \left((1-\alpha)p^+, \frac{q'^2}{2(1-\alpha)p^+} \right)$$

Outlook



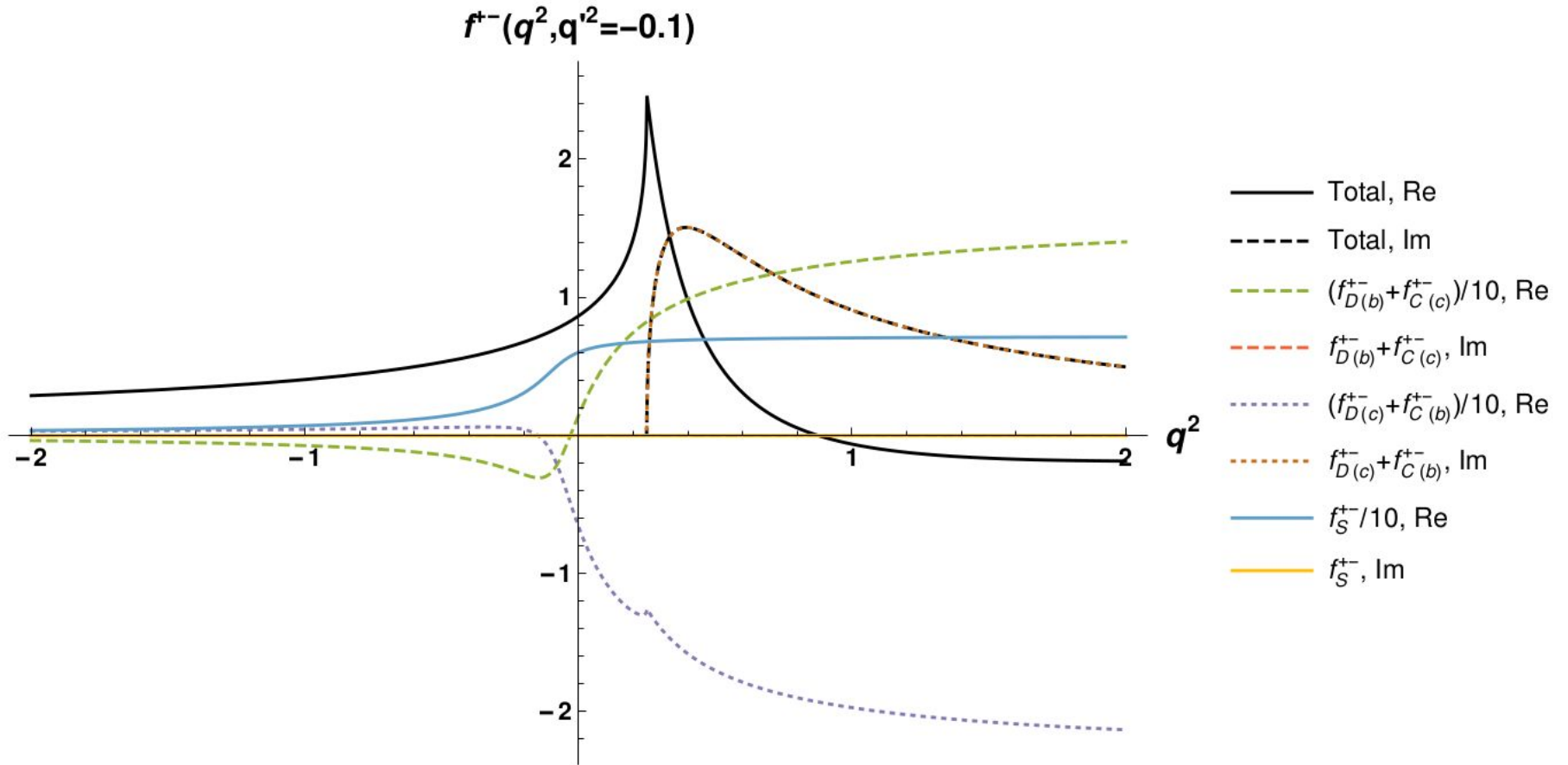
- Assuming $\Gamma_i^{\mu\nu} = f_i(q^2, q'^2) (g^{\mu\nu} q \cdot q' - q'^\mu q^\nu)$, where the index i means each individual Light-Front Time-Ordered (LFTO) diagram, we calculated the contributions from each LFTO diagrams to the form factor.

Outlook



The numerical results of individual x^+ -ordered contributions to the form factor for the case of $m = 0.25 \text{ GeV}$, $M = 0.14 \text{ GeV}$, and $q'^2 = -0.1 \text{ GeV}^2$, normalized to $F(q^2 = 0, q'^2 = 0) = 1$, by picking the $++$ component of the current. Note that $f_{D(b)}^{++} = f_{C(c)}^{++}$ and $f_{D(c)}^{++} = f_{C(b)}^{++}$.

Outlook



The numerical results of individual x^+ -ordered contributions to the form factor for the case of $m = 0.25 \text{ GeV}$, $M = 0.14 \text{ GeV}$, and $q'^2 = -0.1 \text{ GeV}^2$, normalized to $F(q^2 = 0, q'^2 = 0) = 1$, by picking the $+-$ component of the current. Note that $f_{D(b)}^{+-} = f_{C(c)}^{+-}$ and $f_{D(c)}^{+-} = f_{C(b)}^{+-}$.

Outlook

- This shows that each individual LFTO contribution to the form factor depends on which component one takes to make the calculation.
- Each individual contribution in our case is Valence(V) versus Non-Valence (NV), but in other scenarios, e.g. proton mass decomposition calculation, it may be like, quark contribution, gluon contribution, angular momentum contribution, etc. contributions to the $T^{\mu\nu}$ tensor.
- Our theoretical simulation shows that for each individual contribution, one cannot assume it is gauge invariant, and there may be more than one form factor in this case. Only when one adds all the contributions together, the total result is gauge invariant with only one form factor.



Thank you!